

Generation of widely tunable continuous-wave terahertz radiation using a two-dimensional lattice of nonlinear metallic nanodimers

R. E. Noskov* and A. A. Zharov

Institute for Physics of Microstructures, Russian Academy of Sciences, Nizhny Novgorod 603950, Russia

M. V. Tsarev

N.I. Lobachevsky State University of Nizhny Novgorod, Nizhny Novgorod 603950, Russia

(Received 19 February 2010; revised manuscript received 19 May 2010; published 9 August 2010)

We propose an alternative technique of continuous-wave terahertz radiation generation based on light scattering by a two-dimensional flat lattice of nonlinear metallic nanodimers. We show that it may be accompanied by plasmon-driven modulation instability of the lattice polarization resulting in periodic oscillations of both transmitted and reflected light envelopes. We find that the modulation frequency lies in the terahertz band and can be tuned within a wide range, from units up to several tens of terahertz, by varying of the incident light intensity and frequency. We also compare the suggested method with traditional one based on optical heterodyne downconversion.

DOI: [10.1103/PhysRevB.82.073404](https://doi.org/10.1103/PhysRevB.82.073404)

PACS number(s): 42.79.Hp, 78.66.Bz, 71.45.Gm, 75.60.Ej

Great interest to the investigation of light interaction with isolated metallic nanoparticles and nanoparticle arrays is caused, in particular, by plasmonic effects which bode a lot of promising applications in nanophotonics, near-field optics, nanowaveguiding, optical lithography, biosensorics, etc.¹⁻³ To date, sufficient progress in fabrication of well-ordered two-dimensional (2D) and three-dimensional lattices of metallic nanoparticles has been achieved,⁴⁻⁶ that makes possible experimental demonstration of such intriguing optical effects as negative refraction⁷ and cloaking.⁸ Special interest concerns nonlinear plasmon-driven phenomena in such structures. The strong nonlinear optical response of metallic nanoparticles arising due to intraband and interband electron transitions is well known^{9,10} and used for frequency conversion,¹¹⁻¹³ determination of optical field enhancement¹⁴ and high-resolution near-field imaging.^{15,16} However, despite some advances in this realm, the rich potential of nonlinear optical metamaterials for practical applications remains obscure.

Recently, we considered the light scattering by an individual nonlinear metallic nanodimer consisting of a pair of identical spherical metallic nanoparticles.¹⁷ We showed that this scattering may be accompanied by plasmon-driven modulation instability resulting in a periodic self-modulation behavior of the scattered light envelope with the modulation frequency lying in the terahertz band. Bearing in mind that the modulation frequency can also be tuned by variation in incident radiation intensity, it seems very attractive to use arrays of nanodimers as a tunable parametric source of terahertz radiation. In this Brief Report, we just analyze, as an example, light scattering by a two-dimensional flat lattice of such nanodimers embedded into a dielectric substrate (with dielectric permittivity ϵ_s and thickness b) close to the interface illuminated by the pump light, as shown in Fig. 1. Assuming that the radii of particles a and the distance between their centers in dimers d are much smaller than the wavelength of the propagating electromagnetic wave, we treat nanoparticles as point dipoles. Quasielectrostatic coupling between particles produces four collective plasmon eigen-

modes of the dimer: two dipole (longitudinal and transverse) and two quadrupole (also longitudinal and transverse).¹⁷ The dipole-type plasmons of the dimer have finite electric dipole moments and zero magnetic dipole moment. The transverse quadrupole mode has zero electric dipole moment and finite magnetic dipole moment. Both electric and magnetic dipole moments of the longitudinal quadrupole mode equal to zero.

As long as interparticle interaction in the dimer is small, all eigenfrequencies of these modes are close to the frequency of dipole surface plasmon of an individual particle ω_0 . At the same time, dimer excitation at the frequency lying in the vicinity of ω_0 inevitably leads to the resonant growth of the local electric field intensity inside nanoparticles. As a result, one may expect the strong nonlinear response providing nonlinear coupling between dimer eigenmodes. For considered spherical nanoparticles this nonlinearity has a Kerr type,^{9,10} so that its nonlinear dielectric constant can be written as $\epsilon_m^{NL} = \epsilon_m^L(\omega) + \kappa\chi^{(3)}|E|^2$, where $\epsilon_m^L(\omega)$ is the linear term;

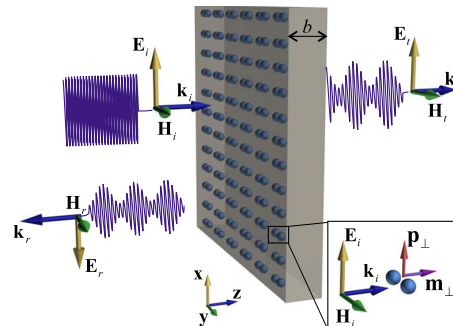


FIG. 1. (Color online) Schematic sketch demonstrating light scattering by a two-dimensional lattice of nonlinear metallic nanodimers in a self-modulation regime. Inset shows electrical dipole moment \mathbf{p}_\perp of the dimer transverse dipole eigenmode excited by the incident wave and magnetic dipole moment \mathbf{m}_\perp of the dimer transverse quadrupole eigenmode excited due to plasmon-driven instability of the dimer transverse dipole eigenmode. Indexes “i,” “r,” and “t” correspond to incident, reflected, and transmitted waves, respectively.

\mathbf{E} is the local electric field tension inside the particles; $\chi^{(3)}$ is the cubic susceptibility of particles; κ indicates the type of nonlinearity:¹⁸ focusing ($\kappa=+1$) and defocusing ($\kappa=-1$). Since we will consider the system only in a very narrow spectral range close to ω_0 , we employ simple Drude model for describing the linear part of permittivity, i.e., $\varepsilon_m^L(\omega)=1-\omega_p^2/[\omega(\omega-i\nu)]$, where ω_p is the electron plasma frequency; ν is the electron scattering rate; ω is the frequency of incident light [$\sim\exp(i\omega t)$]. Within description of $\varepsilon_m^L(\omega)$ by means of Drude formula, the frequency of the fundamental dipole plasmon of an individual particle can be expressed as $\omega_0=\omega_p/\sqrt{1+2\varepsilon_s}$.¹⁷

For our calculations we chose silver nanodimers with $a=10$ nm and $d=30$ nm immersed into the SiO_2 substrate with $\varepsilon_s=2.1$. In the wavelength range of 390–410 nm Drude parameters of silver have the following approximated values $\hbar\omega_p=7.17$ eV and $\hbar\nu=0.12$ eV.¹⁹ The measurements of the resonant nonlinear response of silver nanoparticle aggregates showed that particles with radii 10 nm have $\chi^{(3)}\approx 3\times 10^{-9}$ esu.¹⁰ The type of nonlinearity essentially depends on a dielectric host. For the considered case of the SiO_2 host matrix $\kappa=-1$.²⁰

In the chosen geometry (see Fig. 1), the linearly polarized light is normally incident onto the square lattice of nanodimers so that electric \mathbf{E}_i and magnetic \mathbf{H}_i fields are directed along x and y axes, respectively. We note that in this case the incident wave excites in dimers only the transverse dipole eigenmode with electric dipole moment \mathbf{p}_\perp . However, the transverse quadrupole mode with magnetic dipole moment \mathbf{m}_\perp can also be excited due to nonlinear coupling between these modes.¹⁷ Therefore the transverse quadrupole mode must be also taken into account.

Small size of particles along with small lattice constant in comparison with the wavelength allow us to consider the array of dimers as superposition of effective electrical $\mathbf{j}_s^{(e)}$ and magnetic $\mathbf{j}_m^{(e)}$ surface currents, which can be written as $\mathbf{j}_s^{(e)}=\partial\mathbf{P}_\perp/\partial t=i\omega\mathbf{P}_\perp$ and $\mathbf{j}_m^{(e)}=\partial\mathbf{M}_\perp/\partial t=i\omega\mathbf{M}_\perp$, where \mathbf{P}_\perp and \mathbf{M}_\perp are the lattice electric and magnetic surface polarization densities, respectively. We leave beyond consideration interaction between dimers in the lattice because it is much weaker than interparticle interaction inside dimers as long as the lattice constant l is big enough to consider the system as the lattice of clusters, but not particles. So lattice electric and magnetic surface polarization densities can be written as $\mathbf{P}_\perp=N\mathbf{p}_\perp$ and $\mathbf{M}_\perp=N\mathbf{m}_\perp$, respectively, where $N=1/l^2$ is the surface dimer concentration in the lattice. Under accepted approximations, reflectance $R=E_r/E_i$ and transmittance $T=E_t/E_i$ of the structure can be obtained from boundary conditions for the tangential components of electric and magnetic fields on the left ($z=0$) and the right ($z=b$) interfaces of the substrate²¹

$$\begin{aligned} [E_x]_{z=0} &= 0, & [H_y]_{z=0} &= (4\pi/c)j_{sx}^{(e)}, & [E_x]_{z=b} &= 0, & [H_y]_{z=b} \\ & & & & & & = 0, \end{aligned} \quad (1)$$

where c is the speed of light, square brackets mean the jump of corresponding components of electric and magnetic fields. We note that the magnetic surface current does not produce the discontinuity of E_x because of the absence of the tangen-

tial component (see the inset in Fig. 1). Equations (1) yield the following expressions for R and T :

$$\begin{aligned} R &= R_{sub} + (4\pi/c)[j_{sx}^{(e)}/E_i]\zeta, & T &= T_{sub} - (4\pi/c)[1/(n_s+1)] \\ & \times [j_{sx}^{(e)}/E_i], \end{aligned} \quad (2)$$

where $\zeta=[n_s-1+(n_s+1)\exp(-i2k_s b)]/[(n_s-1)^2-(n_s+1)^2 \times \exp(-i2k_s b)]$, $n_s=\sqrt{\varepsilon_s}$, $k_s=(\omega/c)n_s$, $R_{sub}=(n_s^2-1)[\exp(-i2k_s b)-1]/[(n_s-1)^2-(n_s+1)^2\exp(-i2k_s b)]$ and $T_{sub}=1+R_{sub}(n_s-1)/(n_s+1)$ are the reflectance and transmittance of the substrate without the lattice.²²

In order to get the nonlinear relation between $j_{sx}^{(e)}$ and E_i , we employ dynamical equations for slow varying amplitudes of p_\perp and m_\perp at the frequency close to ω_0 derived in our recent paper, Ref. 17, which in terms of dimensionless units for the considered geometry can be written as follows:

$$-id\tilde{p}_\perp/d\tau + (\Omega + \delta\Omega_L + \delta\Omega_{NL} - i\gamma_{in})\tilde{p}_\perp + \delta W_{NL}\tilde{m}_\perp = \tilde{E}_d, \quad (3a)$$

$$-id\tilde{m}_\perp/d\tau + (\Omega - \delta\Omega_L - \delta\Omega_{NL} - i\gamma_{in})\tilde{m}_\perp - \delta W_{NL}\tilde{p}_\perp = 0, \quad (3b)$$

where $\tilde{p}_\perp=p_\perp/\beta$, $\tilde{m}_\perp=m_\perp(4c)/(\omega_0 d\beta)$, $\beta=\sqrt{8\varepsilon_s^2(1+2\varepsilon_s)/\chi^{(3)}a^3}$, $\tau=\omega_0 t$, $\tilde{E}_d=\tilde{E}_i+\tilde{E}_r$ is the dimensionless amplitude of electric field acting on dimers, $\tilde{E}_{i,r}=\xi E_{i,r}$, $\xi=-3\varepsilon_s/[8\sqrt{2(1+2\varepsilon_s)^3}\cdot\sqrt{\chi^{(3)}}]$, $\Omega=(\omega-\omega_0)/\omega_0$ is the relative operating frequency shift from the resonance value, $\delta\Omega_L=3\varepsilon_s^2/[2(1+2\varepsilon_s)](a/d)^3$ and $\delta\Omega_{NL}=\kappa(|\tilde{p}_\perp|^2+|\tilde{m}_\perp|^2)$ characterize the linear and nonlinear mode eigenfrequency shifts because of quasioleostatic coupling between nanoparticles in the dimer and the effect of field self-influence, respectively, $\gamma_{in}=\nu/(2\omega_0)$ is responsible for thermal losses in particles, $\rho=2\pi a^2 N$ is the surface filling factor which determines the surface portion of metal in the unit cell. The term $\delta W_{NL}=\kappa(\tilde{p}_\perp\tilde{m}_\perp^*-\tilde{p}_\perp^*\tilde{m}_\perp)$ describes a nonlinear energy exchange between transverse dipole and quadrupole eigenmodes. According to Eqs. (2), $E_r=R_{sub}E_i+(4\pi/c)j_{sx}^{(e)}\zeta$. Substituting this expression into Eq. (3a) and identifying $(4\pi/c)j_{sx}^{(e)}\zeta$ as radiation losses of the lattice, we come to the following set of equations:

$$\begin{aligned} -id\tilde{p}_\perp/d\tau + [\Omega + \delta\Omega_L + \delta\Omega_{NL} - i(\gamma_{in} + \gamma_{rad})]\tilde{p}_\perp + \delta W_{NL}\tilde{m}_\perp \\ = (1 + R_{sub})\tilde{E}_i, \end{aligned} \quad (4a)$$

$$-id\tilde{m}_\perp/d\tau + (\Omega - \delta\Omega_L - \delta\Omega_{NL} - i\gamma_{in})\tilde{m}_\perp - \delta W_{NL}\tilde{p}_\perp = 0, \quad (4b)$$

where $\gamma_{rad}=(3/4)\varepsilon_s^2/(1+2\varepsilon_s)a(\omega_0/c)\rho\zeta$ is responsible for radiation losses of the lattice. Equations (2) and (4) form the self-consistent set that defines temporal dynamics of the reflection and the transmission coefficients of the two-dimensional lattice of nonlinear metallic nanodimers illuminated by linearly polarized light with $\omega\sim\omega_0$ at normal incidence (see Fig. 1).

One of the stationary solutions of Eqs. (4) answering to the zero initial conditions is $\tilde{m}_\perp^{(0)}=0$ and $\tilde{p}_\perp^{(0)}\neq 0$ which satisfies the equation $[-i(\gamma_{in} + \gamma_{rad}) + \Omega + \delta\Omega_L]\tilde{p}_\perp^{(0)} + \kappa|\tilde{p}_\perp^{(0)}|^2\tilde{p}_\perp^{(0)}$

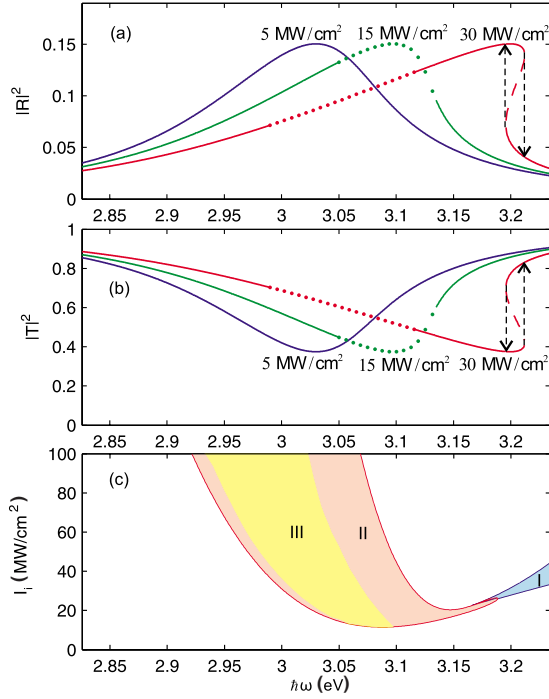


FIG. 2. (Color online) (a) Reflection and (b) transmission spectra for the considered nanostructure at different intensities of the incident wave. Dashed and dotted curves depict the branches which are unstable with respect to small perturbations of P_{\perp} and M_{\perp} , respectively. (c) The regions of electric (I) and magnetic (II+III) instabilities in the plane of incident wave parameters “intensity-frequency.” Areas (II) and (III) indicate zones of magnetic instability growth leading to stationary and self-modulation regimes, respectively. For the considered case (silver nanodimers in the SiO₂ host) $\hbar\omega_0=3.14$ eV. We assumed $l=73$ nm and $b=\pi/k_s$.

$=(1+R_{sub})\tilde{E}_i$. In this case the dependency $\tilde{p}_{\perp}^{(0)}(\tilde{E}_d)$ demonstrates typical for nonlinear oscillators²³ hysteresis behavior at $|\Omega+\delta\Omega_L|>\sqrt{3}[\gamma_{in}+\gamma_{rad}]$ and $\kappa(\Omega+\Omega_L)<0$, that means emerging of a bistability region in the reflection and the transmission spectra when $|\tilde{E}_i|^2>|\tilde{E}_i^{cr}|^2=-\kappa(\Omega+\delta\Omega_L)/[\gamma_{in}+\gamma_{rad}]$ [see Figs. 2(a) and 2(b)]. The middle branches in the hysteresis regions [dashed curves in Figs. 2(a) and 2(b)] are unstable with respect to small perturbations of \tilde{p}_{\perp} and never realize. Besides this, stationary solution can also be unstable with respect to small perturbations of \tilde{m}_{\perp} . The corresponding bands where this instability takes place are depicted in Figs. 2(a) and 2(b) by dotted curves. For brevity we will call these types of instability as electric and magnetic ones, respectively.

Figure 2(c) shows the regions of electric and magnetic instabilities in the “incident light intensity I_i vs light frequency” axes (regions I and II+III, respectively). While the electric instability leads the system either to one or another stable branch in the bistability region [Figs. 2(a) and 2(b)] keeping $\tilde{m}_{\perp}=0$, the magnetic one has two possible scenarios of growth. (1) The system comes to the new steady state with finite both electric and magnetic polarization densities that can be treated as spontaneous magnetization of the lattice [region II in Fig. 2(c)] and (2) the growth of instability results in the undamped periodical oscillations of both \tilde{p}_{\perp} and

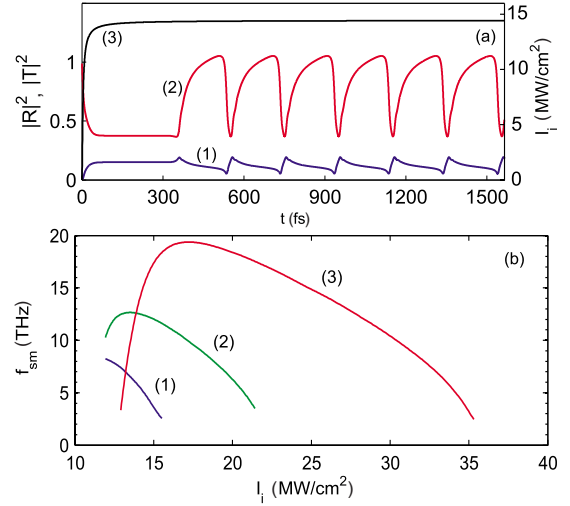


FIG. 3. (Color online) (a) The time dependences of reflectance (1) and transmittance (2) of the 2D lattice of nonlinear silver nanodimers embedded in SiO₂ host during the instability growth at $\hbar\omega=3.091$ eV. Curve (3) shows the temporal dependence of I_i , slowly growing with the saturation value $I_i^{sat}=14.44$ MW/cm². (b) Dependences of the fundamental harmonic of the self-oscillations f_{sm} on I_i at the different incident light frequencies: (1) $\hbar\omega_1=3.091$ eV; (2) $\hbar\omega_2=3.081$ eV; (3) $\hbar\omega_3=3.066$ eV. Lattice parameters are the same as in Fig. 2.

\tilde{m}_{\perp} , causing a self-modulation regime of light scattering by the lattice [region III in Fig. 2(c)].

One of realizations of the second scenario is shown in Fig. 3(a). The intensity of the incident wave is supposed to be slowly growing with the saturation value I_i^{sat} lying in the region III [Fig. 2(c)]. The key features of this continuous-wave (cw) dynamical regime are the terahertz modulation frequency f_{sm} and rather high amplitude modulation indexes of both reflected η_r and transmitted η_t waves [for the self-oscillations shown in Fig. 3(a) $f_{sm}=5$ THz, $\eta_r=0.48$ and $\eta_t=0.41$]. Furthermore, numerical analysis of Eqs. (4) shows that f_{sm} can be tuned in an ultrawide band approximately from units up to several tens of terahertz by changing of the relative operating frequency shift from the resonance value and the incident light intensity [see Fig. 3(b)]. We note that due to the possibility of ω_0 varying throughout the visible spectral range by proper selection of the dielectric substrate, the same f_{sm} for any optical frequency of the pumping light can be obtained.

Apparently, one can interpret the self-modulation dynamics of \tilde{p}_{\perp} and \tilde{m}_{\perp} as parametrically excited beating of dimer transverse dipole and quadrupole modes due to a weak nonlinear coupling between those modes describing by the term δW_{NL} in Eqs. (4).

We draw attention to the fact that energy distribution between reflected and transmitted waves essentially depends on the substrate thickness. Here we considered the case of the half-wave substrate ($b=\pi/k_s$) and obtained maximal transmittance. To provide maximal reflectance, one should use a quarter-wave substrate and, for example, the high reflectance mirror on the backside of the substrate. Such configuration, in addition, decreases the threshold of instability as the lat-

tice will be situated in the antinode of the field. Interestingly, the modulation depth weakly depends on b and is approximately the same for both reflected and transmitted waves.

One can also see that modulation instability growth requires quite high intensities of incident light, higher than 10 MW/cm^2 , that would cause thermal damage to the lattice. However, simple estimations based on the equation of thermal balance at such illumination levels show that diffusion cooling of nanoparticles due to the thermal flow into the substrate provides the stationary temperature level (which is reached in several picoseconds after starting of illumination) about 400–500 K, that is much lower than the melting point of silver ($\sim 1233 \text{ K}$). Thus, only substrate heating may cause thermal cracking of the system. To prevent this undesirable effect, one has to provide proper heat-sink cooling (by means, for example, embedding the system in liquid nitrogen).

It is necessary to note that real terahertz sources of this type, as well as traditional cw terahertz sources based on optical heterodyne downconversion,²⁴ will require detection of scattered light. However, contrary to the heterodyne downconversion method whose main problem is selection of a detecting crystal that would provide contradictory requirements such as high nonlinearity, weak dispersion, and low losses together with wide tunability and good phase matching between pumping light and terahertz harmonics, the suggested technique is much more flexible. Indeed, on the one hand, comparatively low intensities needed for the self-modulation instability growth allow using highly nonlinear

but easily damaged in strong optical fields organic crystals such as BNA (Ref. 25) or DAST (Ref. 26) for terahertz envelope detection. On the other hand, the possibility of terahertz radiation generation with any required ω and f_{sm} by proper selection of the incident light intensity and the dielectric substrate makes possible to fulfill the phase matching condition for much wider types of detector crystals, than heterodyne downconversion. All this along with the ability of f_{sm} tuning in a very wide range manifests that the cw terahertz source based on two-dimensional arrays of nonlinear metallic nanodimers makes a competitive alternative to traditional ones based on optical heterodyne downconversion.

In conclusion, we have shown that light scattering by a two-dimensional lattice of nonlinear metallic nanodimers can be accompanied by plasmon-driven instability of the electric lattice polarization. This effect may lead to the cw self-modulation regime of light scattering with the modulation frequency lying in the terahertz band. We have calculated the conditions for the instability arising and found that the modulation frequency can be tuned from units up to several tens of terahertz by variation in the incident light frequency and intensity. Obtained results show that 2D arrays of nonlinear metallic nanodimers may be considered as the basis for the perspective widely tunable cw terahertz sources.

Authors thank Russian Fund for Basic Research for support through the Grants No. 08-02-00379 and No. 09-02-00863. R.N. also acknowledges the Dynasty Foundation.

*nanometa@gmail.com

¹S. A. Maier, *Plasmonics: Fundamentals and Applications* (Springer, New York, 2007).

²*Optical Properties of Nanostructured Random Media*, edited by V. M. Shalaev (Springer, Berlin, 2002).

³*Near-Field and Surface Plasmon-Polaritons*, edited by S. Kawata (Springer, Berlin, 2001).

⁴A. N. Grigorenko, A. K. Geim, H. F. Gleeson, Y. Zhang, A. A. Firsov, I. Y. Khrushchev, and J. Petrovic, *Nature (London)* **438**, 335 (2005).

⁵N. Liu, H. Guo, L. Fu, S. Kaiser, H. Schweizer, and H. Giessen, *Nature Mater.* **7**, 31 (2008).

⁶M. S. Rill, C. Plet, M. Thiel, I. Staude, G. Freymann, S. Linden, and M. Wegener, *Nature Mater.* **7**, 543 (2008).

⁷J. Valentine, S. Zhang, T. Zentgraf, E. Ulin-Avila, D. A. Genov, G. Bartal, and X. Zhang, *Nature (London)* **455**, 376 (2008).

⁸I. I. Smolyaninov, V. N. Smolyaninova, A. V. Kildishev, and V. M. Shalaev, *Phys. Rev. Lett.* **102**, 213901 (2009).

⁹F. Hache, D. Ricard, C. Flytzanis, and U. Kreibig, *Appl. Phys. A: Solids Surf.* **47**, 347 (1988).

¹⁰V. P. Drachev, A. K. Buin, H. Nakotte, and V. M. Shalaev, *Nano Lett.* **4**, 1535 (2004).

¹¹M. Lippitz, M. A. van Dijk, and M. Orrit, *Nano Lett.* **5**, 799 (2005).

¹²M. W. Klein, C. Enkrich, M. Wegener, and S. Linden, *Science* **313**, 502 (2006).

¹³M. W. Klein, M. Wegener, N. Feth, and S. Linden, *Opt. Express*

15, 5238 (2007).

¹⁴P. J. Schuck, D. P. Fromm, A. Sundaramurthy, G. S. Kino, and W. E. Moerner, *Phys. Rev. Lett.* **94**, 017402 (2005).

¹⁵M. Danckwerts and L. Novotny, *Phys. Rev. Lett.* **98**, 026104 (2007).

¹⁶S. Palomba and L. Novotny, *Nano Lett.* **9**, 3801 (2009).

¹⁷A. A. Zharov, R. E. Noskov, and M. V. Tsarev, *J. Appl. Phys.* **106**, 073104 (2009).

¹⁸The introduction of parameter κ makes sense only when $\text{Re } \chi^{(3)} \gg \text{Im } \chi^{(3)}$.

¹⁹P. B. Johnson and R. W. Christy, *Phys. Rev. B* **6**, 4370 (1972).

²⁰R. A. Ganeev, A. I. Ryasnyansky, A. L. Stepanov, and T. Usmanov, *Phys. Solid State* **46**, 351 (2004).

²¹L. D. Landau and E. M. Lifshitz, *Electrodynamics of Continuous Media* (Pergamon, Oxford, 1984).

²²The alternative technique for calculation of reflectance and transmittance of thin films in terms of the surface electric polarization can be found in the book D. V. Sivukhin, *Optics* (Nauka, Moscow, 1985) (in Russian).

²³M. I. Rabinovich and D. I. Trubetskov, *Oscillations and Waves in Linear and Nonlinear Systems* (Kluwer, Dordrecht, 1989).

²⁴*Terahertz Optoelectronics*, edited by V. Sakai (Springer, Berlin, 2005).

²⁵K. Miyamoto, S. Ohno, M. Fujiwara, H. Minamide, H. Hashimoto, and H. Ito, *Opt. Express* **17**, 14832 (2009).

²⁶H. Ito, K. Suizu, T. Yamashita, A. Nawahara, and T. Sato, *Jpn. J. Appl. Phys.* **46**, 7321 (2007).